IJBPAS, October, 2015, 4(10), Special Issue: 1270-1280
ISSN: 2277–4998

International Journal of Biology, Pharmacy and Allied Sciences (IJBPAS)
'A Bridge Between Laboratory and Reader'
www.ijbpas.com

EFFECT OF MELAMINE-FUNCTIONALIZED MAGNETITE NANOPARTICLES AND POLY (XANTHONE-AMIDE) ON THE CORROSION PROPERTY OF EPOXY RESIN

NEZAM BEYGMOHAMMADI[1], GHASEM RAHPAIMA[1*,] AHMAD KHABBAZI HABIBI[2]

1: Department of Chemistry, Islamic Azad University, Lamerd Branch, Lamerd, Iran

2: Assistant professor at Islamic Azad University, Lamerd Branch, Lamerd, Iran

***Corresponding Author: E Mail: G.rahpaima@iaulamerd.ac.ir, Telfax: +987152720293**

ABSTRACT

In this study, to prepare a high-performance epoxy resin with chemical and corrosion stability, Poly (xanthon-amide) was used to cure diglycidylether of bisphenol-A (DGEBA)-based epoxy resin and blend of DGEBA with functionalized Fe_3O_4 nanoparticles. The corrosion performance of epoxy coated carbon steel was examined by potentiodynamic polarization and weight loss measurements, along with immersion test in, 3.5% NaCl solution and seawater. The results showed that epoxy resins cured with Poly (xanton amide) had low tendency to corrosion. In addition, the cured epoxy resin containing 5% Fe_3O_4 had higher anticorrosion activity than bare DGEBA system. The results showed that functionalized Fe_3O_4 nanoparticles improved anticorrosion activity of the epoxy resin.

Keywords: DGEBA, Poly (xanthon-amide), Corrosion, Stainless steel, Polarization

INTRODUCTION

One of the main issues in industries is the metal corrosion to prevent from which there is no infrastructural action, seriously. The consequence of metal corrosion would be a large economic loss which is to be paid by owners of the industries directly or indirectly. The metal corrosion phenomenon can be defined as a chemical or electrochemical reaction between a material and its surrounding environment which leads to material properties alteration. This phenomenon occurs in all material (metals, ceramic, polymers and composites), but it is more prevalent in metals and results in more damaging effects. Destruction, erosion and corrosion of the materials are due to the

natural processes and causes large losses worldwide, annually. Between 3.5 to 5% of the domestic gross production of the countries is lost, annually [1]. The coastal areas of southern Iran particularly the Asaluyeh zone are ranked in C5M based on the ISO-12944 classification. In such zones, the steel is corroded between 80-200 μm annually. Considering the concentration of petrochemical industries complexes in Mahshahr and Asaluyeh and large amount of investments, protecting these plants for long term exploitation would be of significant importance [2]. In order to reduce the corrosion economic effects, the corrosion engineers supported by the scientists in this field are attempting to reduce the material waste and economic costs due to the pipes, tanks, metallic elements of the machineries, ships, bridges and marine plants corrosion and like that. For this purpose, in order to maintain the internal and external surfaces of the equipment and tankers against the corrosion there have been different methods for improvement of the corrosion stability of metals among which glazing is one of the most common metal protection methods against corrosion. The protecting layers and covers are used for different purposes and the important target is to separate the metal from the surrounding environment. The covers usually are used for corrosion stability, erosion stability, electrical insulators and appearance. Generally, the covers are divided into 3 classes: organic, mineral and metallic covers. The covers are composed of these 3 types are very common and are known as composite or hybrid covers [3]. Epoxy is one of the most frequently used organic covers for protecting the surface of steel against corrosion. The high networking density and adhesiveness of epoxy is the reason it is very stable against corrosion. The organic covers due to prevention from electrolyte penetration to the joint surface of metal and cover can play the role of anti-corrosion [4]. Poly Xanthons are polymers with high performance which at least have a xanthon chain in each repeating unit. Poly Xanthons are strong and stable against the attacks of most of solvents; chemicals and UV ray and represents good physical and electrical properties in high temperature. Also, its derivatives provide an anti-corrosion property as a cocking factor [5]. Also, poly amides are used alone or along with epoxy resins is suitable cover for protecting different metals [6]. In order to manufacture the Nano-composites, different polymer matrices are used. Also, the diversity of minerals used for manufacturing Nano-composites is very extensive; each system is designed for particular applications and objectives considering the produced Nano-composite properties [7-10]. Environmental factors effective

on the corrosion rate are different depending on the sea water depth. The alteration of such factors in different zones seas water is collected in scientific sources. The main effective factor in steel corrosion in sea water is the available oxygen level which varies between 6 ppm to 11 ppm. The solubility of oxygen in sea water is influenced by salinity and temperature. Therefore, as temperature increases, the rate of corrosion would be affected by adverse influences due to the oxygen in the sea water steel [11]. In this paper, poly (xanthon-amide) is used as a cocking factor in order to obtain a suitable cover for stainless steel and the cocked resin's anti-corrosion activity in presence and lack of presence of iron-functionalized magnetic Nano-particles also is accurately assessed.

Experimental section

Used tools and equipment

All the corrosion and electrochemical experiments were performed using a Potentiostate/Galvanostate µAutolab3, made in Netherland, equipped with PGSTAT30 and NOVA 1.5 software which is controlled by PC. A 3-electrode electrochemical cell including a saturated calomel electrode (SCE), platinum rod and stainless steel 304 were used as reference electrode, assistant electrode and working electrode, respectively.

Chemicals

The chemicals used in this research were bought from Floca and Merc and were applied without any purification.

The stainless steel used in this study

The considered steel in this research is stainless steel 8-18 ((%18Cr-%8Ni) which is a low alloy steel of standard type ASTM A-304. As it is revealed from the name, its significant feature is chromium stability in acidic medium which prevents from metal corrosion.

Preparing the required solutions

NaCl 5.3% solution

100 ml of NaCl 3.5% with 3.5g NaCl dissolve in 100 mL distilled water was prepared.

The Fe_3O_4 functionalized magnetic Nanoparticles synthesis

In a bi-opening 50 mL balloon equipped with magnetic stirring and cooling, 0.2g (0.74 mM) of $FeCl3.H_2O$ and 0.5g Sodium citrate in 10 mL ethylene glycol were dissolved. Then 6g Melamine was added to the solution. The reaction mixture was stored in 220 ˚C for 6 hours. After completion of the reaction, the solid products were isolated using magnetic filtration and were washed by water without ion and pure ethanol several times. The final product was dried in 100 ˚C vacuum oven for 6 hours.

Table1. The steel chemical component, the elements' value in term of weight percentage

W	Ti	V	Ni	Cr	Cu	Co	Mo	Mn	Fe	S.S GR. B
2%	0.7%	11%	8.14%	18.83%	0.42%	9%	0.24%	1.023%	71.45%	MAT. 304

Stainless steel sample preparing

Preparing the steel sample is performed in a way that the middle section of the blade is completely and the lower section partly are covered with lac so that they would be in touch with the intra-cell solution. The laced section is dried by air. In the following, the uncovered section of the steel sample is smoothed by sandpaper. In order to de-grease the sample was washed by acetone and until the covering process it was stores in a closed vessel.

Poly (xanthon-amide) synthesis

In order to prepare the polyamides the phosphorylation method is applied. In a 500 ml bi-opening balloon equipped with a magnetic stirring, re-flax cooling, thermo-meter and inlet and outlet pipe for nitrogen gas, a mixture of di-amine DAX, Octanoic di-acid, phenyl phosphate, pyridine, lithium chloride were added to 15 ml NMP under nitrogen gas. The reaction mixture was un-der nitrogen gas in 100 ˚C for 12 hours. Then the reaction mixture was poured in large amount of methanol and the deposit obtained was filtered and washed by a mix-ture of hot methanol and water. For more purification, the synthesized polymer was experimented in methanol for 12 hours. The product was dried in vacuum oven in 80 ˚C for 48 hours and the overall yielding for PXAO synthesis was about 85% (1g). The FT-IT spectrum data and proton spectrum are consistent with PXAO structure [12-14].

PXAO: FTIR (KBr, cm^{-1}): 3350, (NH), 3072 (C-H, Ar), 1660 (C=O), 1110 (C-O)

^1H NMR (400 MHz, DMSO-d_6): δ 10.20 (S, 2H, NH), δ 8.43-8.46 (m, 2H, CH), δ 7.90-7.98 (m, 2H, CH), δ 7.53-7.59 (m, 2H, CH), δ 2.30-2.34 (m, 4H, CH_2), δ 1.61-1.65 (m, 4H, CH_2), δ 1.30-1.33(m, 4H, CH_2).

The procedure of investigating the steel blade corrosion by software

The polarization TOFEL tests and electrochemical experiments were performed by the Potentios-tate/Galvanostate μAutolab3 and based on the typical 3-electrode system,. At first of every experiment, in order to obtain open circuit potential condition (OCP) or metal corrosion potential (E_{corr}), the working elec-trode, i.e. the sample of steel obtained, was floated in the experiment solution. Potenti-odynamic polarization curves were recorder with automatic potential alteration in range of ±250 mV relative to corrosion or OCP and with rate of 5 $mV.s^{-1}$ and in similar temperature conditions (room temperature). Using NOVA 1.5 software, the polarization curves were analyzed and the its TOFEL

area was identified and manipulated to the corrosion potential and the corrosion current (I_{corr}) would be obtained. The already prepared solution (as a corroding medium) in electrochemical cell after the OCP condition is met using above program, the TOFEL polarization diagrams were obtained and recorded. The procedure is in a manner that after pouring 25 ml from polarization curves in both mediums, the NaCl 3.5% solution and the Persian Gulf water in uncovered steel electrode and covered electrode by poly xanthon and melamine-iron nanoparticle protected are recorded.

DISCUSSION

Identification of poly (xanthon-amide): PXAO

PXAO was identified after being synthesized in spectrometry approaches such as FT-IR and H NMR. The FT-IR spectrum indicates the index absorption composition in 3350 cm^{-1} related to amine N-H strain vibration, in 3072 cm^{-1} related to aromatic C-H, in 1660 cm^{-1} related to C=H carbonyl and in 1110 cm^{-1} related to C-O group (figure1) and H NMR spectrum of this composition indicates the index of amide hydrogen in 10.20 ppm and aromatic protons in range 1.33- 7.99 ppm (figure2).

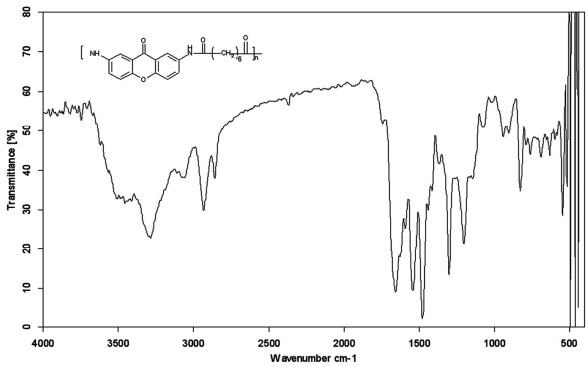

Figure1. Poly (xanthon-amide) (PXAO) FT-IR spectrum

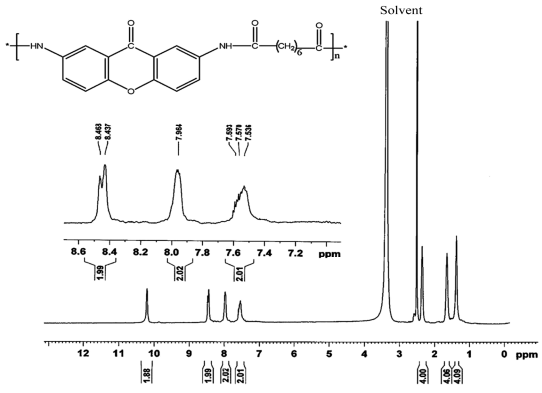

Figure2. Poly (xanthon-amide) (PXAO) H NMR spectrum

Identification of Fe_3O_4 functionalized magnetic nanoparticles

Fe_3O_4 functionalized magnetic nanoparticles after being synthesized by different spectrometry approaches such as XDR, FT-

IR were identified. The FT-IR spectrum of this composition indicates the bifurcate index peak in 3400 cm^{-1} related to amine NH_2 symmetric and asymmetric strain vibration and index peak in 1500-1600 cm^{-1} related to C=N (figure3) and XRD spectrum indicates the crystal structure of nanoparticles (figure6).

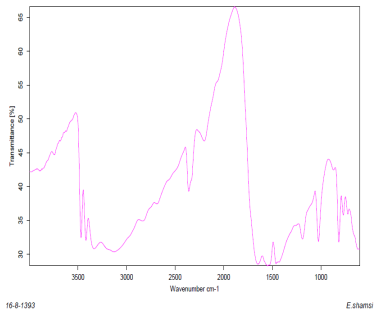

Figure3. Fe_3O_4 functionalized magnetic nanoparticles FT-IR spectrum

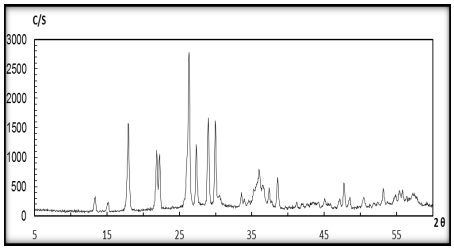

Figure4. Fe_3O_4 functionalized magnetic nanoparticles XRD spectrum

Assessment of stainless steel corrosion in salt solution

Figures 5 and 6 indicate steel TFFEL and linear polarization stability diagram and curve in NaCl 3.5% medium, for a linear zone around corrosion potential. Using E_{corr} diagram of steel in NaCl 3.5% solution of -0.2706, the Anode and cathode TOFEL gradients of 1.04×10^{-3} and 9.5293×10^{-3} are obtained. Polarization stability is calculated from the slope of TOFEL polarization diagram (scheme 1) where ΔE is the voltage variability for applied current (I_{app}).

$$R_p = \left(\frac{\Delta E}{\Delta i}\right)_{\Delta E \to 0}$$

Scheme1. Calculation of polarization stability from TOFEL polarization diagram slope

In practice, calculating R_p of the polarization curve or in other word the curve of potential alterations relative to current density for a linear zone around the corrosion potential is depicted in order to obtain a straight line whose slope would be polarization stability in term of $\Omega.cm^2$ and its intercept would be the corrosion potential. Also, R_p can be converted to the corrosion density using Stern-Geary equation [15].

$$I_{corr} = \frac{\beta_a \beta_c}{2.3(\beta_a + \beta_c)R_p}$$

Scheme2. Stern-Geary equation

Where β_a and β_c are anode and cathode gradients of TOFEL diagram, respectively. The ratio of $\frac{\beta_a \beta_c}{2.3(\beta_a+\beta_c)R_p}$ is known as Stern-Geary constant. Using relation 3, the corrosion rate (C.R) would be calculated in term of mills per year (mpy) [16]:

$$C.R = 0.0129 \times \frac{M}{n} \times \frac{1}{\rho} \times i_{corr}$$

Shceme3. Corrosion rate in term of mpy

Where M is the metal atomic weight for iron of 55.85 $g.mol^{-1}$, ρ is the stainless steel density of 7.86$g.cm^{-3}$ and n is metal capacity in corrosion which for iron is 2 [16]. In figure 5, there straight line of equation: y=108450x-0.2705 indicates that consider-

ing the explanations of section 2.8.1, the slope of this line is R_p equal to 108450 $\Omega.cm^2$. by substitution of the values in equation 2 and 3, the density of current and corrosion rate can be calculated or necessary information would be read from the device. Order data obtained 2.24×10^{-7} $\mu A.cm^{-2}$ and 1.12×10^{-8} mpy.

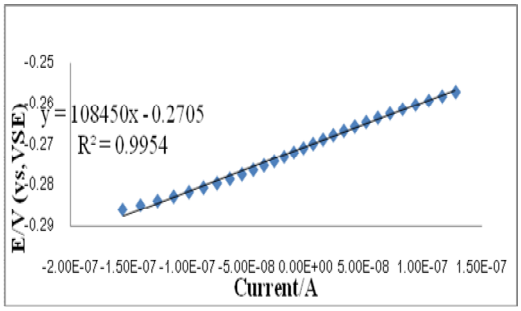

Figure5. Linear polarization diagram of steel in NaCl 3.5% medium

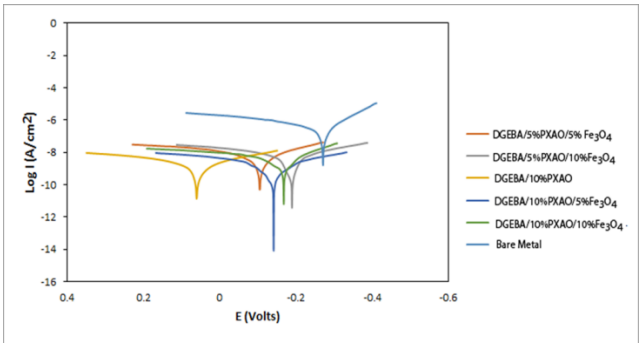

Figure6. Curve of 6 epoxy protecting layer samples based on poly (xanthon-amide) and nanoparticles of melamine-iron (s.s/PXAOS/N) in NaCl 3.5% medium

Table1. Results of steel and epoxy protecting cover corrosion based on melamine-iron and poly (xanthon-amide) in NaCl 3.5% medium

%C.R (mpy)	%Pef	I corr (μ A cm2-)	Ecorr (V vs, SCE)	Rp(Ω.cm2)	Bc(v.dec-1)	Ba(v.dec-1)	cover
1.12×10^{-9}	0	2.44×10^{-7}	-2.70×10^{-1}	1.08×10^{5}	3.33×10^{-1}	8.27×10^{-2}	Metal in NaCl
1.33×10^{-9}	98.8	2.90×10^{-9}	-1.88×10^{-1}	2×7^{10}	3.21×10^{-1}	2.29×10^{-1}	R+%5P+%10 F
6.99×10^{-11}	99.4	1.53×10^{-9}	-1.40×10^{-1}	4×7^{10}	2.40×10^{-1}	3.38×10^{-1}	R+%10P+%5F
1.71×10^{-10}	98.4	4.02×10^{-9}	-1.68×10^{-1}	1×7^{10}	1.28×10^{-1}	3.35×10^{-1}	R+%10P+%10F
2.18×10^{-10}	98.1	4.76×10^{-9}	-1.05×10^{-1}	1×7^{10}	1.75×10^{-1}	2.93×10^{-1}	R+%5P+%5F
6.68×10^{-11}	99.2	1.89×10^{-9}	5.93×10^{-2}	3×7^{10}	2.35×10^{-1}	2.95×10^{-1}	R+%10P
%C.R (mpy)	$\%P_{ef}$	I_{corr} (μ A cm2-)	E_{corr} (V vs, SCE)	R_p(Ω.cm2)	B_c(v.dec-1)	B_a(v.dec-1)	Cover

R: Epoxy resin; P:PXAO; F:Fe_3O_4

As it is observed from table 1, the percentage of protection for epoxy cover with melamine-iron nanoparticles is more protective than poly xanton epoxy protecting layer. Considering the table it is seen that the curve related to sample with Fe_3O_4 functionalized magnetic nanoparticle relative to DGEBA/PXAO has more positive corrosion potential and this potential for both samples of (steel) without protecting layer is more positive.

Assessment of steel 304 corrosion in Persian Gulf water

Figure 7 shows the steel polarization stability in sea water for a linear zone around the corrosion potential. Using corrosion po-

tential TOFEL diagram for the steel in sea water of -32436v, the anode and cathode TOFEL gradients are 1.40×10^{-1} and 67% are obtained, respectively. Also, a straight line with the equation: y=29622x-0.3244 is indicated which considering the explanations of section 2.8.1 the slope of this line is R_p which is equal to 29622 Ω.cm□.

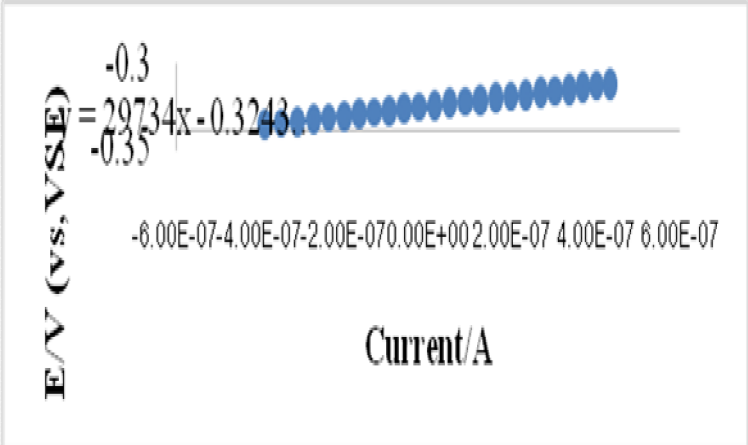

Figure7. S.S metal linear polarization stability curve in Persian Gulf water

Assessment and comparison between steel 304 corrosion with poly xanthon and melamine nanoparticle covers in Persian Gulf water

Figure 8 indicates the poly epoxy protecting cover TOFEL diagrams on the basis of poly xanthon and melamine-iron nanoparticles in sea water in comparison to each other. The related curve to melamine-iron nanoparticles has more positive corrosion potential than epoxy cover based on poly xanthon and the corrosion potential of both samples is more positive than steel without cover. These results indicate that the effect of epoxy cover and melamine modified nanoparticles play the role of protection against corrosion.

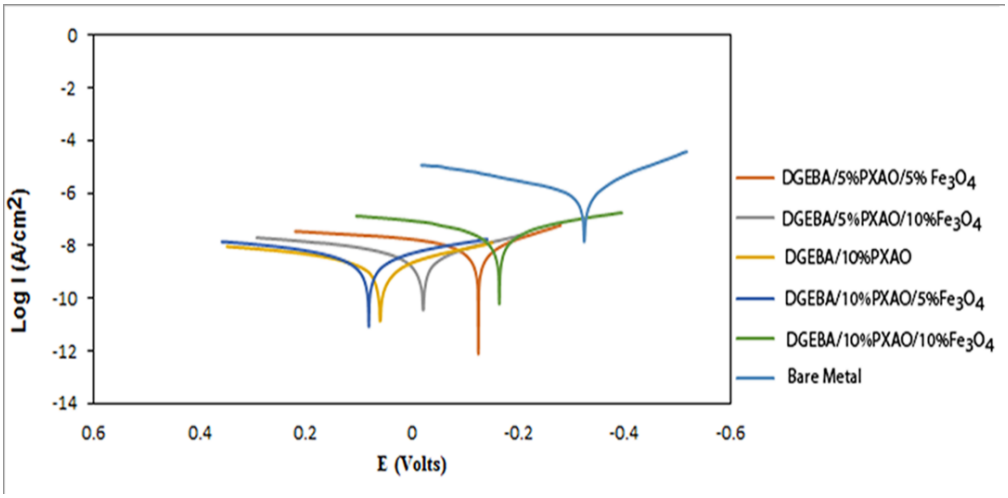

Figure9. Stainless steel and epoxy protecting cover based on poly xanthon and melamine-iron nanoparticles TOFEL curve in Persian Gulf water

Table2. Results of the steel corrosion calculation and protective epoxy cover based on poly xanthon and melamine-iron nanoparticles in Persian Gulf water

%C.R (mpy)	$\%P_{ef}$	I_{corr} (μ A cm2-)	E_{corr} (V vs, SCE)	R_p(Ω.cm2)	B_c(v.dec-1)	B_a(v.dec-1)	Cover
6.04×10^{-8}	0	1.32×10^{-6}	-3.24×10^{-1}	2.97×10^{4}	1.32×10^{-1}	2.86×10^{-1}	Sea water
2.86×10^{-10}	99.6	5.86×10^{-9}	-2.13×10^{-2}	1×10^{7}	2.22×10^{-1}	3.42×10^{-1}	%5P+%10 F
1.73×10^{-10}	99.71	3.76×10^{-9}	8.20×10^{-2}	2×10^{7}	3.06×10^{-1}	4×10^{-1}	R+%10P+%5F
1.81×10^{-9}	97.01	3.95×10^{-8}	-1.64×10^{-1}	2×10^{6}	3.18×10^{-1}	4.27×10^{-1}	R+%10P+%10F
3.99×10^{-10}	99.31	8.70×10^{-9}	-1.24×10^{-1}	5×10^{6}	1.54×10^{-1}	2.86×10^{-1}	R+%5P+%5F
9.38×10^{-11}	99.8	2.05×10^{-9}	5.94×10^{-2}	3×10^{7}	2.41×10^{-1}	3.41×10^{-1}	R+%10%P
%C.R (mpy)	$\%P_{ef}$	I_{corr} (μ A cm2-)	E_{corr} (V vs, SCE)	R_p(Ω.cm2)	B_c(v.dec-1)	B_a(v.dec-1)	Cover

R: Epoxy resin; P: PXAO; F:Fe_3O_4

Sample weight reduction measurement in in Persian Gulf water

In this research, in order to investigate the corrosion rate, the stainless steel weight reduction, the epoxy protecting cover on the poly xanthon and melamine-iron nanoparticles basis were floated in sea water in laboratory temperature after 15 days and the weight reduction is calculated by:

$$IE = \left(\frac{W_{free} - W_{add}}{W_{free}}\right) \times 100$$

Scheme5. Sample weight reduction measurement formal

Where IE is the sample weight percentage, Wfree is the sample weight prior to floating and Wadd is the sample weight after floating. Considering the calculations performed the epoxy cover weight reduction percentage equals 83% and the epoxy cover of melamine-iron nanoparticles equals 91%.

Comparison between steel corrosion studied in salt, Persian Gulf water

In figure 10, the steel TOFEL diagrams are compared in both mediums which considering the positivity of corrosion potential of the diagram of salt water is it understood that corrosion occurs more in more salty sea water.

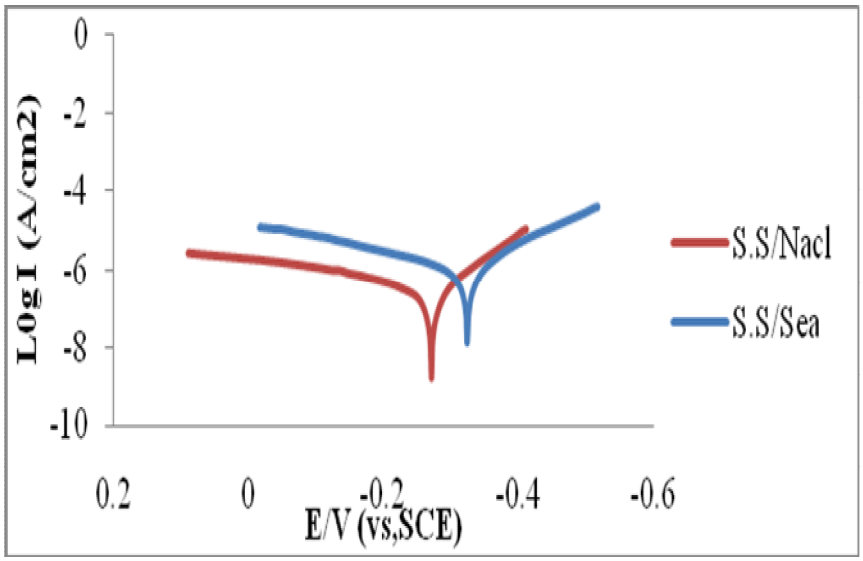

Figure10. Comparison between steel corrosion studied in sea water, NaCl 3.5%

CONCLUSION

In this research, the melamine-iron nanoparticle and poly xanthon cocked covers' performance was investigated in stainless steel surface as a stable coverage against corrosion in both salt water 3.5% and Persian Gulf water. Considering the obtained TOFEL diagrams and calculations performed based on the Potentiodynamic polarization curves it was detected that the poly xanthon epoxy protecting cover can lower the corrosion rate, but the melamine-iron nanoparticles epoxy cover lowers this rate more than the former one. These results indicate the suitable stability of cocked epoxy resin cover against corrosion and shows that they can be used in corroding mediums.

REFERENCES

[1] Kassiriha, S.M. Standard Guideline of Surface Preparation and Application of Protective Coatings, ICA, 2007 U Tehran-Iran.

[2] Kassiriha, S.M. Phanomen farbe, April 2010.

[3] Sim chi, A(2008), "introduction to nanoparticles (properties, production process and applications), volume 1, tehran: scientific publication institute of Sharif industrial University, p. 265, pp. 19-36.

[4] Ramezanzadeh B, Attar M., An evaluation of the corrosion resistance and adhesion properties of an epoxy-nanocomposite on a hot-dip galvanized steel (HDG) treated by different kinds of conversion coatings, Surface & Coating Technology205, 2011, 4649- 4657.

[5] Mehdipour-ataei, S. (2005). Naphthalene-ring containing diamine and resulting thermally stable polyamides.European Polymer Journal,41(9), 2887–2892.

[6] Okamoto, M. (2006). Recent advances in polymer/layered silicate nanocomposites: an overview from science to technology.Material Science Technology, 22(7) 756-779.

[7] Goitisolo, I., Eguiazábal, J. I., & Nazabal, J. (2010). Stiffening of poly (ethylene terephthalate) by means of polyamide 6 nanocomposite fibers produced during processing. Composites Science and Technology, 70(5), 873–878.

[8] Mansoori, Y., Sanaei, S. S., Zamanloo, M., & Atghia, S. V. (2013). Synthesis and Properties of New Polyimide / Clay Nanocomposite Films. Bulletin Material Science, 36(6), 789-798.

[9] Lu, X., Zhang, W., Wang, C., Wen, T., & Wei, Y. (2011). Progress in

Polymer Science One-dimensional conducting polymer nanocomposites: Synthesis, properties and applications. Progress in Polymer Science, 36(5), 671–712

[10] Li, J., Zhou, C., & Gang, W. (2003). Study on nonisothermal crystallization of maleic anhydride grafted polypropylene/montmorillonite nanocomposite.*Polymer Testing*, *22*, 217–223.

[11] V. S. Sastri, Edward Ghali, Mimoun Elboujdaini. 2007. Corrosion Prevention and Protection Practical Solutions. England: Published by John Wiley & Sons Ltd, The Atrium, Southern Gate, Chichester, West Sussex PO19 8SQ, PP: 207-246.

[12] Smejkal CW, Vallaeys T, Burton SK, Lappin-Scott HM (2001) Lett. Appl Microbiol., 32: 273.

[13] Husain A, Nami SAA, Siddiqi KS (2010) J. Mol. Struct., 970:117.

[14] Yamazaki N, Higashi F, Kawataba J (1974) J Polym. Sci. Polym. Chem. Ed., 12:2149.

[15] A. Poursaee, Cement and Concrete Research 40 (2010) 1451–1458.

[16] ASTM G102-89, (2004), Standard Practice for Calculation of Corrosion Rates and Related Information from Electrochemical Measurements, Annual Book of ASTM Standards, Vol. 03.02, 2006, 7 pp.